

Induced Attenuation of Scleral TGF- β Signaling in Mutant Mice Increases Susceptibility to IOP-Induced Optic Nerve Damage

Magdalena Gebert, Johanna Heimbucher, Valentina K. Gsell, Kristof Keimer, Andrea E. Dillinger, and Ernst R. Tamm

Institute of Human Anatomy and Embryology, University of Regensburg, Regensburg, Germany

Correspondence: Magdalena Gebert, Institute of Human Anatomy and Embryology, University of Regensburg, Universitätsstraße 31, Regensburg D-93053, Germany; magdalena.gebert@ur.de.

Received: August 7, 2023

Accepted: January 11, 2024

Published: January 31, 2024

Citation: Gebert M, Heimbucher J, Gsell VK, Keimer K, Dillinger AE, Tamm ER. Induced attenuation of scleral TGF- β signaling in mutant mice increases susceptibility to IOP-induced optic nerve damage. *Invest Ophthalmol Vis Sci.* 2024;65(1):48. <https://doi.org/10.1167/iovs.65.1.48>

PURPOSE. Axonal optic nerve (ON) damage in glaucoma is characteristically associated with increased amounts of active transforming growth factor-beta 2 (TGF- β 2) in the ON head. Here we investigated the functional role of scleral TGF- β signaling in glaucoma.

METHODS. A deficiency of *Tgfb2*, which encodes for TGF- β receptor type II (TGF- β RII), the essential receptor for canonical TGF- β signaling, was induced in fibroblasts (including those of the sclera) of mutant mice. To this end, 5-week-old mice were treated with tamoxifen eye drops. Experimental glaucoma was induced in 8-week-old mice using a magnetic microbead (MB) model. After 6 weeks of high intraocular pressure (IOP), the ON axons and their somata in the retina were labeled by paraphenylenediamine (PPD) and RNA-binding protein with multiple splicing (RBPMS) immunohistochemistry, respectively, and quantified.

RESULTS. Tamoxifen treatment resulted in a significant decrease of TGF- β RII and its mRNA in the sclera. After 6 weeks of high IOP, reduced numbers of PPD-stained ON axons were seen in MB-injected eyes in comparison with not-injected contralateral eyes. Moreover, MB injection also led to a decrease of retinal ganglion cell (RGC) somata as seen in RBPMS-stained retinal wholemounts. Axon loss and RGC loss were significantly higher in mice with a fibroblast specific deficiency of TGF- β RII in comparison with control animals.

CONCLUSIONS. We conclude that the ablation of scleral TGF- β signaling increases the susceptibility to IOP-induced ON damage. Scleral TGF- β signaling in mutant mice appears to be beneficial for ON axon survival in experimentally induced glaucoma.

Keywords: sclera, TGF- β signaling, experimental glaucoma, optic nerve, retinal ganglion cells

Glaucoma, the second leading cause for blindness worldwide,^{1,2} is characterized by the continuous loss of optic nerve (ON) axons. Glaucomatous damage occurs at the optic nerve head (ONH), where retinal ganglion cell (RGC) axons exit the eye.³⁻⁵ Data from multiple randomized prospective multicenter studies show that intraocular pressure (IOP) is the main risk factor for the onset and progression of glaucoma.⁶⁻¹¹ The reasons for the degeneration of ON axons in glaucoma are incompletely understood.

Degeneration of ON axons in glaucoma is associated with a continuous rearrangement of the connective tissue elements in the ONH. The changes cause cupping of the ONH, a typical clinical observation in affected patients.^{3,12-14} In addition, the peripapillary sclera (PPS) surrounding the ONH changes as its fibrillar extracellular matrix (ECM) rearranges, and its stiffness increases significantly.^{15,16}

The structural changes of ONH and PPS correlate with a marked increase of transforming growth factor-beta 1 (TGF- β 1) and TGF- β 2 in the ONH and aqueous humor of glaucoma patients.¹⁷⁻¹⁹ TGF- β is a signaling molecule with

myriad functions. Both TGF- β 1 and TGF- β 2 are stored in the extracellular matrix in an inactive form and can be released and activated following an increase in tissue strain.²⁰⁻²² As a consequence, active TGF- β induces the formation of fibrillar ECM, thereby changing its biomechanical properties.

IOP likely modulates stress and strain in the sclera resulting in increased availability of active TGF- β upon high IOP. This scenario could well explain the high amounts of active TGF- β in the ONH of patients with glaucoma. It appears to be reasonable to assume that higher amounts of active TGF- β in the ONH and PPS contribute to the observed structural and biomechanical changes in glaucoma. Up until now, it is unclear, though, if and how the changes contribute to ON axon loss in glaucoma.

Here, we were interested in learning about the specific function of scleral TGF- β in glaucoma. To this end, we generated mutant mice with an induced deficiency of *Tgfb2* in fibroblasts. *Tgfb2* encodes for the TGF- β receptor type II (TGF- β RII) which is the essential receptor for canonical TGF- β signaling. Our results indicate that the reduction of scleral

TGF- β signaling increases the vulnerability of ON axons and RGC somata in experimental glaucoma induced by increased IOP. The molecular changes induced by higher amounts of active TGF- β in the PPS appear to protect ON axons from glaucomatous damage.

MATERIAL AND METHODS

Animals and Animal Husbandry

Mice carrying two floxed *Tgfr2* alleles (*Tgfr2^{fl/fl}*) were crossbred with *Tgfr2^{fl/fl}/Col1a2-Cre/ERT* mice heterozygous for a Cre-recombinase transgene that is specifically activated in fibroblasts upon induction with tamoxifen (TX).^{23,24} *Tgfr2^{fl/fl}/Col1a2-Cre/ERT* animals were used as experimental group and designated as *Tgfr2 Δ Sclera*; *Tgfr2^{fl/fl}* littermates served as controls. The genetic background of *Tgfr2^{fl/fl}* mice was 129S1/Sv and that of *Col1a2-Cre/ERT* animals was C57BL/6J. Breeding resulted in a mixed 129S1/Sv-C57BL/6J background for both experimental and control groups. All animal procedures performed in this study complied with the ARVO Statement for the Use of Animals in Ophthalmic and Vision Research and with institutional guidelines. All experiments were approved by the local authorities (Regierung von Unterfranken, RUF, AZ: 55.2-2532-2-734).

Induction of Cre Recombinase

To activate Cre recombinase, which leads to the excision of the floxed *Tgfr2* allele in *Tgfr2 Δ Sclera* animals, experimental animals and their respective control littermates were treated with 10 μ L per eye of TX-containing eye drops (5 mg/mL) at an age of 5 weeks, three times a day for 5 consecutive days, as described previously.²⁵

Microbead Injection and IOP Measurements

Intracameral injection of magnetic microbeads was performed as published previously.²⁶ Mice were anesthetized by an intraperitoneal injection of ketamine-xylazine. After the induction of pupil dilatation using tropicamid eyedrops (Mydriaticum Stulln; Pharma Stulln, Stulln, Germany), 2.4×10^6 beads (Invitrogen Dynabeads M-450 Epoxy; Thermo Fisher Scientific, Waltham, MA, USA) were injected into the anterior chamber of the right eye in a final volume of 3 μ L. The left eye served as an intra-animal control. IOP was measured non-invasively under inhalation anesthesia by isoflurane. Measurements were conducted at the same time of day (8 AM–9 AM) using a TonoLab tonometer (Icare, Vantaa, Finland) and following the manufacturer's recommendations.²⁷ Six measurements were taken and automatically processed by the instrument's software. The average of 4 measurements, excluding the highest and lowest result, was given as final result. Measurements were

repeated if SD was not ≤ 2.5 . IOP was measured directly before microbead injection, 3 d after injection and then in weekly intervals up to 6 wks.

RNA Analysis

Sclerae of experimental and control mice were dissected 2 weeks after treatment with TX. Total RNA of sclerae was extracted with pegGOLD TriFast (VWR, Radnor, PA, USA) according to the manufacturer's recommendations. First-strand cDNA was prepared from total RNA using the qScript cDNA Synthesis Kit (Quantabio, Gaithersburg, MD, USA) according to the manufacturer's instructions. Real-time reverse-transcription polymerase chain reaction (RT-PCR) was performed on an iQ5 real-time PCR detection system (Bio-Rad Laboratories, Hercules, CA, USA) using the following temperature profile: 40 cycles of 10 seconds melting at 95°C and 40 seconds of annealing and extension at 60°C. Primer pairs (Table 1) were purchased from Invitrogen and extended over exon-intron boundaries. RNA that was not reversely transcribed served as negative control for real-time RT-PCR. Receptor for activated C kinase 1 (RACK1) was used as the housekeeping gene for relative quantification of the real-time RT-PCR experiments. Quantification was performed with iQ5 Standard Edition (Version 2.0.148.60623) software (Bio-Rad Laboratories).

Western Blot Analysis

Protein of sclerae was extracted with pegGOLD TriFast according to manufacturer's recommendations, and protein content was measured with the bicinchoninic acid protein assay (Pierce Biotechnology, Rockford, IL, USA). Proteins were separated by sodium dodecyl sulfate-polyacrylamide gel electrophoresis (SDS-PAGE) and transferred to polyvinylidene fluoride membranes. Western blot analysis was performed with specific antibodies as described previously.²⁸ Antibodies were used as follows: rabbit anti-TGF- β R2 (1:1000; Cell Signaling Technology, Danvers, MA, USA), rabbit anti-connective tissue growth factor (CTGF, 1:500; R&D Systems, Minneapolis, MN, USA), Rabbit Anti-Alpha-Tubulin (1:1000; Rockland Immunochemicals, Pottstown, PA, USA), and Goat anti-Rabbit HRP and Goat anti-Rabbit Alkaline Phosphatase (1:2000; Cell Signaling Technology). The intensity of the bands detected by western blot analysis was determined using appropriate software (AIDA Image Analyzer, Elysia Raytest, Straubenhardt, Germany; ImageLab, Bio-Rad Laboratories).

Light Microscopy and Quantification of Optic Nerve Axons

Eyes were enucleated and fixed in Karnovsky's solution (2.5% glutaraldehyde and 2.5% paraformaldehyde [PFA] in 0.1-M cacodylate buffer) for 24 hours. After rinsing in

TABLE 1. Sequences of Primer Pairs Used for RT-PCR

Primer	Species	Orientation	Sequence 5' to 3'	Position
TGF- β R2	<i>Mus musculus</i>	Forward	agaagccgcatgaagtctg	634–652
		Reverse	ggcaaacctctccagagta	686–705
CCN2/CTGF	<i>Mus musculus</i>	Forward	tgacctggaggaaaacattaaga	1013–1035
		Reverse	agccctgtatgtcttcacactg	1124–1103
RACK1	<i>Mus musculus</i>	Forward	tctgcaagtacacggctcag	514–533
		Reverse	gagacgatgatagggttctg	604–584

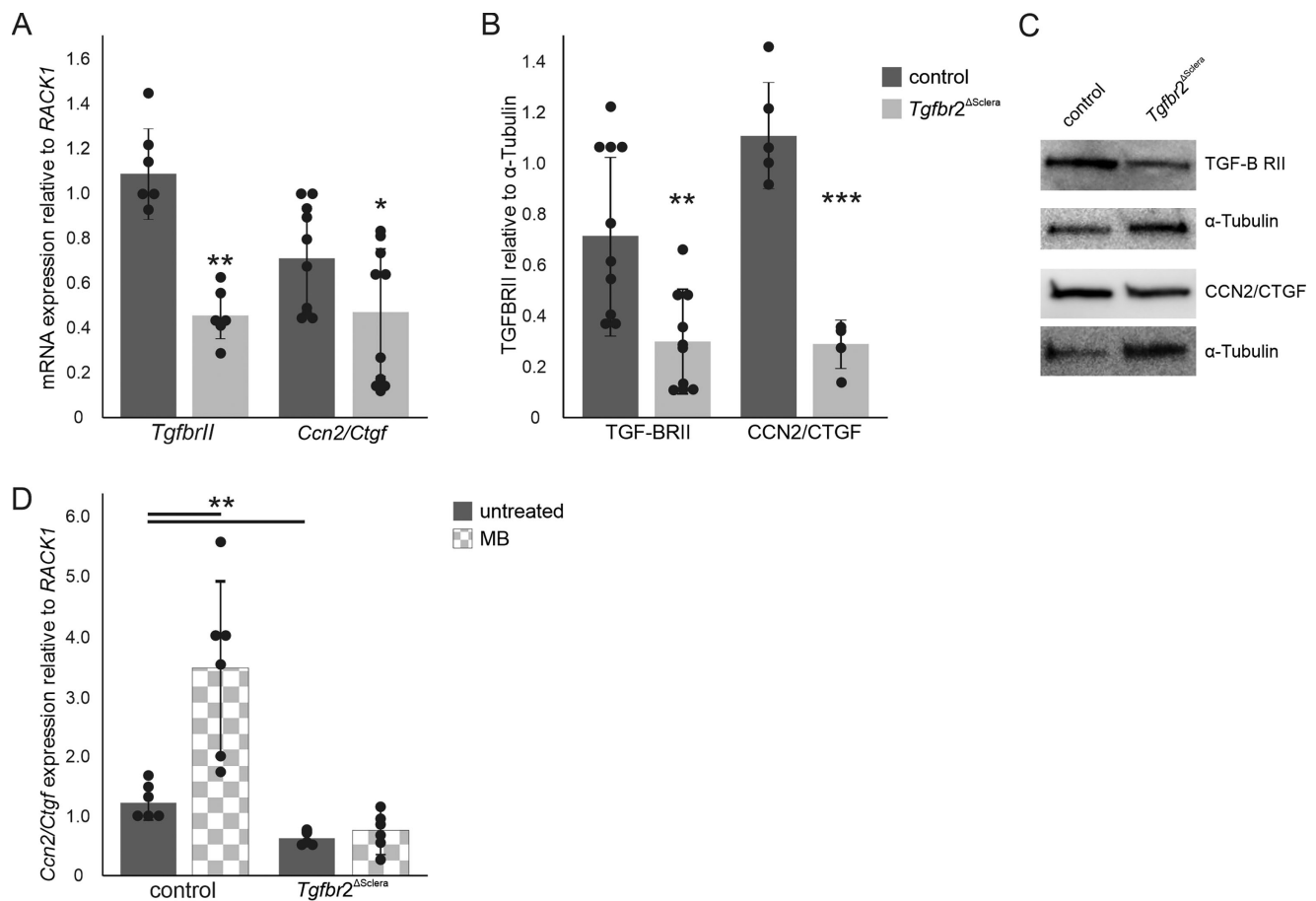


FIGURE 1. TGF- β RII and CCN2/CTGF were reduced in the sclera of *Tgfr2*^{ΔSclera} animals after treatment with TX. **(A)** Real-time RT-PCR of scleral mRNA. Two weeks after the treatment with tamoxifen the expression of *Tgfr11* mRNA and that of its downstream target *Ccn2/Ctgf* was significantly reduced in *Tgfr2*^{ΔSclera} animals compared to control littermates (*Tgfr11*: control, 1.08 ± 0.21 ; *Tgfr2*^{ΔSclera}, 0.45 ± 0.12 ; $P = 0.0001$; $n = 6$; *Ccn2/Ctgf*: control, 0.71 ± 0.24 ; *Tgfr2*^{ΔSclera}, 0.44 ± 0.31 ; $P = 0.044$; $n = 10$). **(B)** Densitometry of western blot analysis for the amounts of TGF- β RII and CCN2/CTGF in scleral proteins. Both were significantly lowered by TX treatment (TGF- β RII: control, 0.72 ± 0.32 ; *Tgfr2*^{ΔSclera}, 0.30 ± 0.19 ; $P = 0.002$; $n = 10$; CCN2/CTGF: control, 1.13 ± 0.21 ; *Tgfr2*^{ΔSclera}, 0.28 ± 0.11 ; $P = 0.0002$; $n = 5/4$). **(C)** Representative western blot for TGF- β RII and CCN2/CTGF in scleral proteins of control and *Tgfr2*^{ΔSclera} animals. For normalization α -tubulin was used. **(D)** Six weeks after injection of MB *Ccn2/Ctgf* mRNA was significantly increased in the sclera of control animals when compared to the sclera of the untreated control eye (control, 1.22 ± 0.26 ; control MB, 3.46 ± 1.47 ; $P = 0.01$; $n = 6$). In contrast, *Ccn2/Ctgf* mRNA was not altered after MB injection in the experimental group (*Tgfr2*^{ΔSclera}, 0.64 ± 0.11 ; *Tgfr2*^{ΔSclera} MB, 0.77 ± 0.37 ; $P = 0.42$; $n = 6$). In addition, 6 weeks after TX treatment, *Ccn2/Ctgf* was significantly reduced in the sclera of untreated eyes of *Tgfr2*^{ΔSclera} animals in comparison with untreated controls (control, 1.23 ± 0.26 ; *Tgfr2*^{ΔSclera}, 0.65 ± 0.11 ; $P = 0.004$; $n = 6$).

0.1-M cacodylate buffer, post-fixation was accomplished in a mixture of 1% osmium tetroxide (OsO_4) and 0.8% potassium ferrocyanide in 0.1-M cacodylate buffer for 2 hours at 48°C. Eyes were then dehydrated in a graded series of ethanol and embedded in EPON (Serva Electrophoresis, Heidelberg, Germany). Myelinated optic nerve axons were visualized by paraphenylenediamine (PPD; Carl Roth, Karlsruhe, Germany) staining of EPON-embedded semithin sections. PPD-stained cross-sections were visualized by brightfield microscopy using a 100 \times oil immersion objective for highest resolution. The area of the optic nerve was measured with AxioVision Viewer 3.0 (Carl Zeiss Microscopy, Oberkochen, Germany).

Optic nerve axons were quantified using AxonCounter, a precise and unbiased stereological sampling scheme implemented as an ImageJ (National Institutes of Health, Bethesda, MD, USA) plugin that was recently developed by us and described previously.²⁹ In short, after calibrating the

image with the scale bar, the area of the optic nerve was measured in square micrometers using ImageJ, and myelinated axons in five fields (50 \times 50 μm^2 each) were counted. The mean density (axons/ μm^2) in each of the five measured regions was multiplied by the total area of the optic nerve to give the estimated total number of axons. Axons were quantified in a blinded manner by two individual observers (MG, KK). Mean values of both counts were used for statistical analysis.

Staining and Quantification of Retinal Ganglion Cells

Eyes were enucleated and fixed in 4% (w/v) PFA in phosphate-buffered saline (PBS) for 15 minutes. Dissected retinæ were stored in 0.1-M PBS overnight at 4°C. The next day the retinæ were fixed in 100% methanol

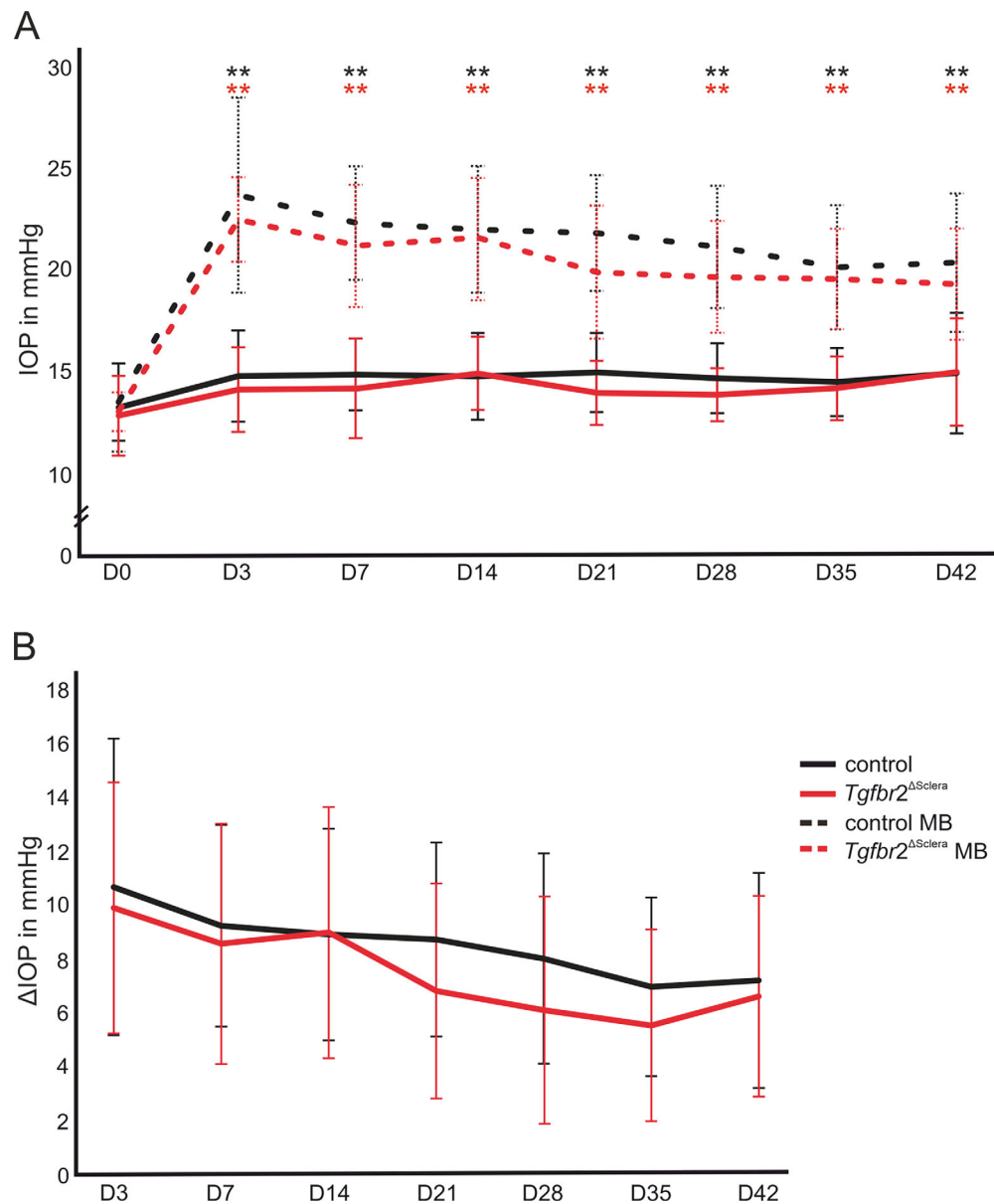


FIGURE 2. IOP was significantly increased after the injection of MBs in control and *Tgfr2* Δ Sclera animals. **(A)** IOP did not differ between control and *Tgfr2* Δ Sclera animals before injections (*Tgfr2* Δ Sclera, 12.03 ± 2.06 ; control, 12.56 ± 2.27 ; $P = 0.39$; $n = 29$ each). After injection, IOP was significantly elevated for the duration of 6 weeks (see Table 2; $n = 29$). **(B)** Δ IOP was not different between control and *Tgfr2* Δ Sclera mice at any time point measured ($n = 29$).

TABLE 2. IOP and Δ IOP Values for Control and *Tgfr2* Δ Sclera Mice Before and After Injection of MBs

Day	Mean \pm SD					
	Control	Control MB	<i>Tgfr2</i> Δ Sclera	<i>Tgfr2</i> Δ Sclera MB	Δ IOP Control	Δ IOP <i>Tgfr2</i> Δ Sclera
D0	12.56 ± 2.27	12.83 ± 1.99	12.13 ± 2.06	12.34 ± 2.11	0.00 ± 0.00	0.00 ± 0.00
D3	14.18 ± 2.35	23.50 ± 5.03	13.48 ± 2.18	22.23 ± 3.67	10.67 ± 5.51	9.89 ± 4.66
D7	14.38 ± 2.35	20.97 ± 2.89	13.80 ± 3.44	21.18 ± 4.94	8.75 ± 3.62	8.27 ± 4.61
D14	14.37 ± 2.04	21.73 ± 3.26	14.32 ± 2.56	21.31 ± 3.94	8.90 ± 3.93	8.97 ± 4.67
D21	14.72 ± 2.41	21.15 ± 3.45	13.18 ± 2.13	19.51 ± 2.69	8.71 ± 3.61	7.14 ± 4.00
D28	14.07 ± 1.80	20.83 ± 3.16	13.21 ± 1.37	19.27 ± 2.87	8.00 ± 3.91	6.95 ± 4.23
D35	13.87 ± 1.76	19.79 ± 3.20	13.55 ± 1.64	19.19 ± 2.30	6.95 ± 3.32	6.87 ± 3.56
D42	14.50 ± 3.18	20.02 ± 3.57	14.64 ± 2.90	18.92 ± 2.47	7.19 ± 4.00	6.60 ± 3.73

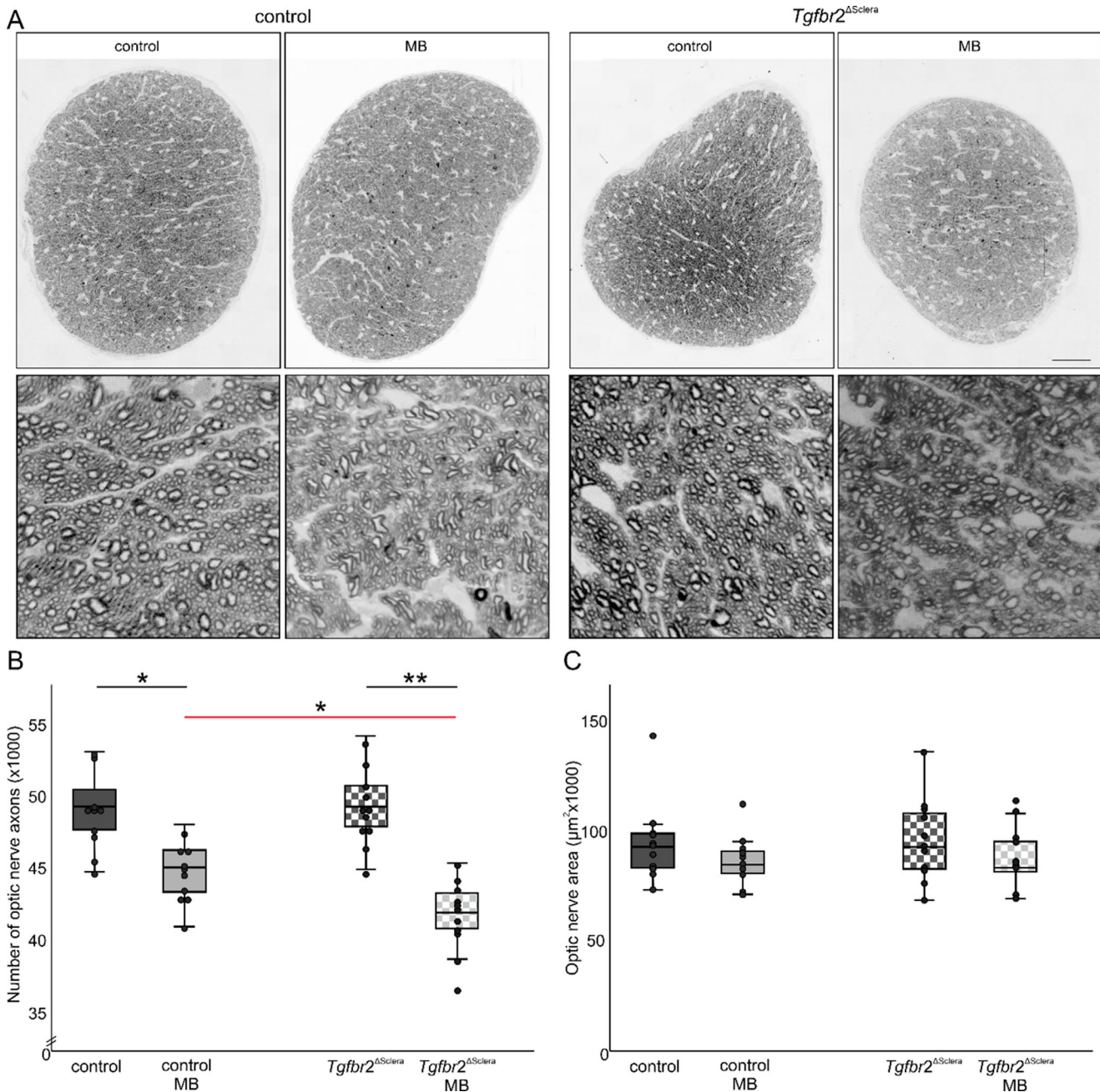


FIGURE 3. Axon loss was significantly increased in *Tgfr2*^{ΔSclera} mice but optic nerve size was not affected by genotype or high IOP. (A) PPD-stained cross-sections of optic nerves used for axon quantification showed no gross morphological differences between the groups. Larger areas devoid of axons and increased numbers of swollen axons were observed in MB eyes of both groups. Scale bars: 50 μm. Higher magnifications show an area of 50 × 50 μm. (B) Axon numbers of not-injected eyes did not differ between control and *Tgfr2*^{ΔSclera} mice (control, 48,686 ± 2644; *Tgfr2*^{ΔSclera}, 49,133 ± 2543; $P = 1.00$; $n = 10/11$), but axon numbers of *Tgfr2*^{ΔSclera} mice were significantly lower after 6 weeks of high IOP than those of control mice (control ocular hypertension, 44,450 ± 4954; *Tgfr2*^{ΔSclera} ocular hypertension, 41,636 ± 2460; $P = 0.028$; $n = 10/11$). (C) ON area was not altered by the ablation of scleral TGF- β signaling or the injection of magnetic MBs (control, 94,498 ± 18,273 μm²; *Tgfr2*^{ΔSclera}, 95,767 ± 19,143 μm²; control MB, 86,149 ± 11,330 μm²; *Tgfr2*^{ΔSclera} MB, 86,914 ± 15,252 μm²; $n = 10/11$).

(MeOH) for 15 minutes at -25°C and then washed three times in 0.1-M PBS for 15 minutes. For antigen retrieval, retinæ were incubated in 0.05-M NH_4Cl for 45 minutes followed by three washing steps in 0.1-M PBS. After blocking with 3% bovine serum albumin (BSA) in tris-buffered saline with 0.1% Triton X-100 for 1 hour at room temperature, RGCs were stained using rabbit

anti-RNA-binding protein with multiple splicing (RBPMS, 1:1000; GeneTex, Irvine, CA, USA) for 2 hours at room temperature (RT). Afterward, the retinæ were washed three times with 0.1-M PBS followed by incubation for 1 hour at room temperature with Cy3 Goat Anti-Rabbit IgG (1:2000, Jackson ImmunoResearch, West Grove, PA, USA). Negative controls were carried out using only secondary antibodies.

TABLE 3. ON Size, Axon Density, and Axon Numbers for Control and Tgfb β 2 Δ Sclera Mice Before and After Injection of MBs

	ON Size (μm^2)	Axons per μm^2	Axon Number	RGC per mm^2
	Mean \pm SD			
Control	94,498 \pm 18,273	0.559 \pm 0.05	48,686 \pm 2644	2206 \pm 175
Control MB	86,149 \pm 11,330	0.501 \pm 0.07	44,450 \pm 1954	1954 \pm 212
Tgfb β 2 Δ Sclera	95,767 \pm 19,143	0.560 \pm 0.08	49,133 \pm 2543	2258 \pm 225
Tgfb β 2 Δ Sclera MB	86,914 \pm 15,252	0.495 \pm 0.09	41,636 \pm 2460	1727 \pm 258
	<i>P</i>			
Control vs. Tgfb β 2 Δ Sclera	1.000	1.000	1.000	1.000
Control MB vs. Tgfb β 2 Δ Sclera MB	1.000	1.000	0.028	0.043
Control vs. control MB	1.000	0.439	0.002	0.025
Tgfb β 2 Δ Sclera vs. Tgfb β 2 Δ Sclera MB	1.000	0.257	0.000	0.000

Bold numbers represent statistically significant *P* values.

After washing three times with 0.1-M PBS, whole retinæ were flatmounted onto glass slides using Cytoation Fluorescent Mounting Medium (Dako, Glostrup, Denmark).

To count the total number of RGCs, the area of the whole retina was measured with AxioVision Viewer 3.0. After calibrating the image with the scale bar, the area of the whole retina was again measured in square micrometers using ImageJ, and the stained RGCs of the whole retina were counted. At least 75% of the retina was analyzed for each sample. RGCs were quantified in a blinded manner by two individual observers (MG, KK), and mean RGC numbers from both quantifications were used for the statistical analysis. RGC numbers were calculated as RGCs/ mm^2 .

Statistical Analysis

Data are expressed as mean \pm SD. Statistical evaluation was performed using SPSS Statistics 26 (IBM, Chicago, IL, USA). Normal distribution of data was ensured using the Kolmogorow–Smirnow test with Lilliefors correction. Student's *t*-test for unpaired data and one-way analysis of variance (ANOVA) were used to evaluate statistical significance. Levels of statistical significance and the numbers for each experiment are indicated in the figure legends.

RESULTS

Induced Deletion of Scleral TGF- β RII and Reduced TGF- β Signaling

To confirm the induced deletion of TGF- β RII, we analyzed its expression in the sclera 2 weeks after TX treatment. *Tgfb β RII* was significantly reduced in Tgfb β 2 Δ Sclera animals in comparison with control littermates (Tgfb β 2 Δ Sclera, 0.45 \pm 0.12; control, 1.08 \pm 0.21; *P* \leq 0.01; *n* = 6) (Fig. 1A). Regarding TGF- β RII, western blot analysis showed a 59% reduction in Tgfb β 2 Δ Sclera mice 2 weeks after induction, corroborating the mRNA results (Tgfb β 2 Δ Sclera, 0.30 \pm 0.19; control, 0.72 \pm 0.32; *P* \leq 0.01; *n* = 10) (Fig. 1B). To analyze if the 55% reduction in TGF- β RII resulted in decreased activity of the TGF- β pathway, we quantified the relative expression of *Ccn2/Ctgf*, a typical downstream target of TGF- β signaling. *Ccn2/Ctgf* was significantly reduced by 50% in experimental animals (Tgfb β 2 Δ Sclera, 0.44 \pm 0.31; control, 0.71 \pm 0.24; *P* \leq 0.05; *n* = 9) (Fig. 1A). CCN2/CTGF protein was also significantly reduced after TX treatment (Tgfb β 2 Δ Sclera, 0.28 \pm 0.11; control, 1.13 \pm 0.21; *P* \leq 0.001; *n* = 5/4) (Fig. 1B). After microbead (MB) injection, the expression of *Ccn2/Ctgf*

significantly increased in control animals. In contrast, no increase was observed in Tgfb β 2 Δ Sclera animals (control, 1.22 \pm 0.26; control MB, 3.46 \pm 1.47, *P* \leq 0.01; Tgfb β 2 Δ Sclera, 0.64 \pm 0.11; Tgfb β 2 Δ Sclera MB, 0.77 \pm 0.37, *P* = 0.42; *n* = 6) (Fig. 1D).

IOP Increase in MB-Injected Mice

Prior to bead injection, IOP did not differ between control and Tgfb β 2 Δ Sclera mice (Tgfb β 2 Δ Sclera, 12.03 \pm 2.06; control, 12.56 \pm 2.27; *P* = 0.39; *n* = 29) (Fig. 2A). IOP was significantly increased from 3 to 42 days after injection of MBs. No difference in IOP was detected between Tgfb β 2 Δ Sclera and control animals at any time point (for IOP values, see Table 2). The increase in IOP (Δ IOP = IOP injected eye – IOP not-injected eye) did not differ between the experimental group and the control group at any time point analyzed (Fig. 2B, Table 2).

Reduced Scleral TGF- β Signaling Increases Loss of Axons and RGCs

High IOP causes loss of RGC axons and somata in experimental glaucoma. Therefore, we quantified PPD-stained RGC axons in optic nerve cross-sections and RGC somata in RBPMS-stained retinal wholemounts of control and Tgfb β 2 Δ Sclera animals 6 weeks after the injection of magnetic MBs. In control animals, 6 weeks of high IOP led to loss of axons (control, 48,686 \pm 2644; control MB, 44,450 \pm 1954; *P* \leq 0.001; *n* = 10), and in Tgfb β 2 Δ Sclera animals the observed loss (Tgfb β 2 Δ Sclera, 49,133 \pm 2543; Tgfb β 2 Δ Sclera MB, 41,636 \pm 2460; *P* \leq 0.001; *n* = 11) was significantly increased (*P* \leq 0.05) (Fig. 3B, Table 3). High IOP had no effect on either ON size or on axon density (axons per μm^2) in control or Tgfb β 2 Δ Sclera mice (Fig. 3C, Table 3).

Staining against RBPMS indicated a decrease of RGCs 6 weeks after MB injection, especially in the periphery (Fig. 4A). Quantification of RBPMS-positive cells showed that, for control animals, the average RGC density (RGCs/ mm^2) was 2206 \pm 175, which decreased to 1954 \pm 212 (86% \pm 9.61%) after 6 weeks of high IOP (*P* \leq 0.001; *n* = 14). In Tgfb β 2 Δ Sclera animals, RGC density decreased from 2258 \pm 225 to 1727 \pm 258 (74% \pm 11.43%; *P* \leq 0.001; *n* = 13). This decrease was significantly higher than in control animals (*P* \leq 0.05) (Fig. 4B).

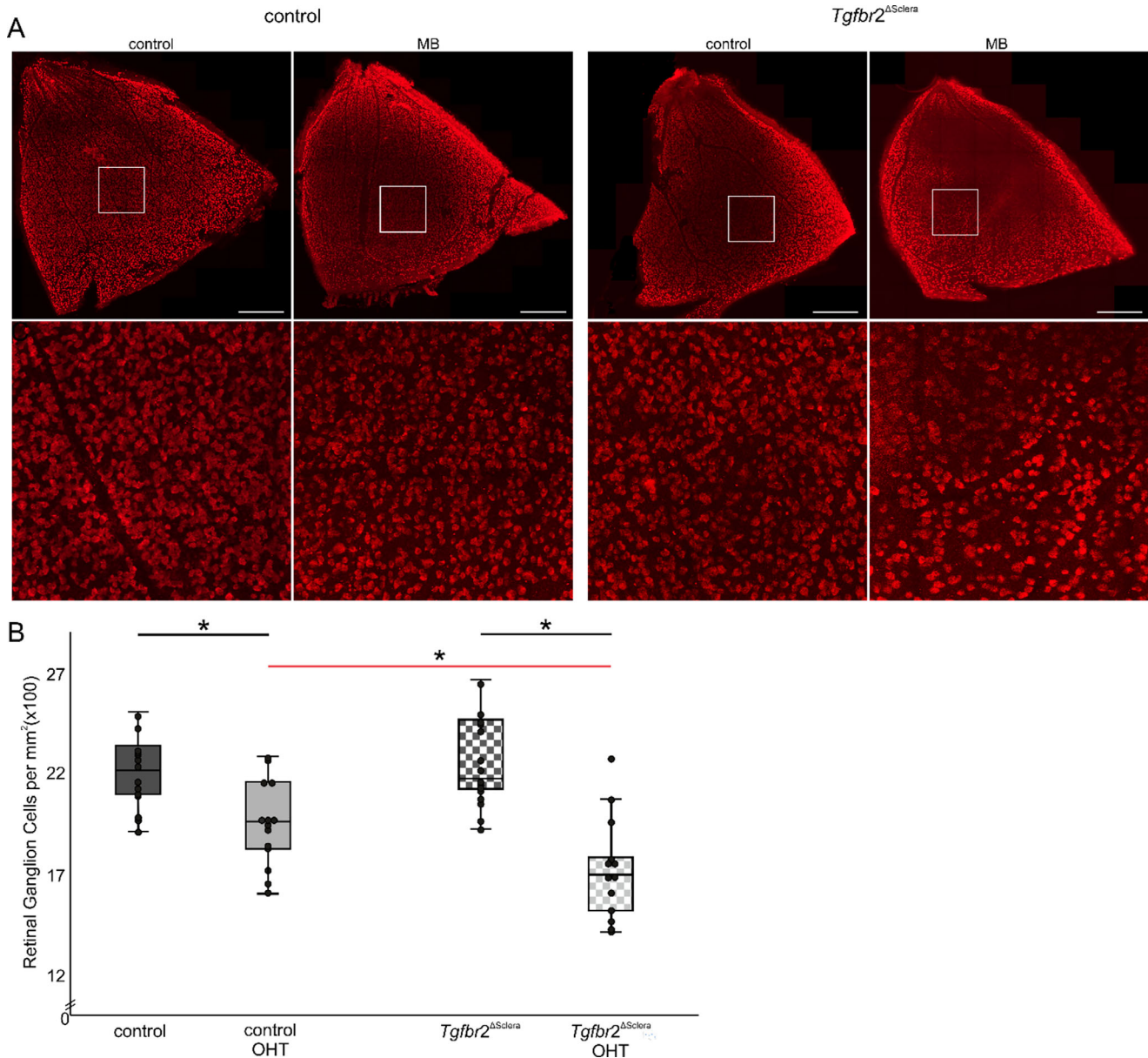


FIGURE 4. RGC loss was elevated in *Tgfr2*^{ΔSclera} mice following MB injection when compared to control littermates. **(A)** Representative images of RBPMs-stained retinas. Scale bars: 500 μ m. Higher magnifications show an area of 500 \times 500 μ m. **(B)** RGC numbers for not-injected eyes did not differ between control and *Tgfr2*^{ΔSclera} mice (control, 2206 \pm 175; *Tgfr2*^{ΔSclera}, 2258 \pm 225; $P = 1.00$; $n = 13$), but RGC numbers for *Tgfr2*^{ΔSclera} mice were significantly lower 6 weeks after MB injection than those of control mice (control MB, 1954 \pm 212; *Tgfr2*^{ΔSclera} MB, 1727 \pm 258; $P = 0.035$; $n = 13$).

DISCUSSION

We conclude that scleral TGF- β signaling protects RGC somata and their axons in the optic nerve from damage caused by high IOP in experimental glaucoma. This conclusion rests on (1) the induced reduction of TGF- β RII and its mRNA in the sclera of *Tgfr2*^{ΔSclera} mice, (2) the generation of high IOP following MB injection, and (3) the significant increase in RGC and axon loss in mice with reduced TGF- β signaling in the sclera.

Currently, the molecular mechanisms behind this protective effect are unclear. Our approach supposedly causes a reduction in canonical TGF- β signaling in all cells with high activity of the *Col1a2* promoter throughout the body.

Commonly, high activity of this promoter is seen in fibroblasts. It appears reasonable to assume that the protective effect against IOP-induced damage in the eye is due to specific functions in scleral fibroblasts that are close to the ONH such as the PPS. As in other dense connective tissues, TGF- β signaling in the sclera induces collagen formation and contractility of fibroblasts. Both scenarios should lead to greater stiffness of the sclera and may be the cause for the greater scleral stiffness that has been observed in glaucoma. Our results appear to indicate that higher scleral stiffness protects ON axons from damage in glaucoma. In this context, it is of interest to note that scleral TGF- β decreases in myopia, leading to reduced ECM production and scleral thickness,^{30–32} and that

patients with myopia have a higher risk for ON damage in glaucoma.^{33–35}

The function of TGF- β in the eye is not restricted, though, to the sclera. In contrast, TGF- β is almost ubiquitously expressed in ocular tissues^{18,36–38} and appears to have a multitude of tissue-specific functions. For example, TGF- β signaling is required for maintenance of retinal and choroidal vessels in the adult or developing eye and attenuates apoptosis of retinal neurons during development.^{39–41} Accordingly, although scleral TGF- β might protect from degeneration in glaucoma, high activity of TGF- β signaling in other ocular cell types might rather promote it. Such effects might explain the observations that treatment of mice with losartan, an inhibitor of the angiotensin 1 (AT1R) receptor, protects from ON degeneration in MB-induced experimental glaucoma.⁴² Losartan suppresses Smad2 phosphorylation and TGF- β expression in its canonical pathway,^{43,44} thereby reducing TGF- β signaling activity. On the other hand, the effects may also be related to other signaling pathways that act downstream of AT1R receptors. In a rat glaucoma-model, a similarly protective effect could be shown for candesartan, a related AT1R inhibitor.⁴⁵

Several potential caveats of this study should be considered: First, it is unclear if the induced deficiency of TGF- β signaling in mutant mice directly affected IOP levels following MB-induced ocular hypertension; if so, was it different than that in the control eyes? Our weekly IOP measurements strongly argue against such a scenario but naturally give no information on the complete IOP history during each of the 42 days following bead injection. Second, rebound tonometry as used in the present study to measure IOP is influenced by the biomechanical properties of the cornea. The induced deficiency of TGF- β signaling may influence those properties. We regard such an effect as unlikely, as in a previous study using the mouse as model⁴² neither normal IOP nor experimentally induced high IOP (measured by Tono-Lab and invasively by cannulation) was affected by losartan, a compound that induces inhibition of TGF- β signaling. Third, axon loss was significant yet small in both groups (9% in the control group vs. 15% in the experimental group) and did not result in significant differences in axon density. Increasing the duration of elevated IOP would likely cause an increase in axon loss and a significant decrease in axon density. Finally, it remains to be shown if the observed effects in murine eyes with an astrocyte-based glial lamina are also relevant for the primate eye with a lamina cribrosa containing numerous connective tissue strands. Nevertheless, identification of the molecular mechanisms that are induced by scleral TGF- β signaling to protect ON axons from damage in murine experimental glaucoma is likely to provide novel insights into the pathogenesis of glaucoma.

Acknowledgments

The authors thank Margit Schimmel, Silvia Babl-Artmann, and Angelika Pach (Institute of Human Anatomy and Embryology, University of Regensburg) for excellent technical assistance.

Disclosure: **M. Gebert**, None; **J. Heimbucher**, None; **V.K. Gsell**, None; **K. Keimer**, None; **A.E. Dillinger**, None; **E.R. Tamm**, None

References

1. Thylefors B, Negrel AD, Pararajasegaram R, Dadzie KY. Available data on blindness (update 1994). *Ophthalmic Epidemiol.* 1995;2(1):5–39.

2. Thylefors B, Negrel AD, Pararajasegaram R, Dadzie KY. Global data on blindness. *Bull World Health Organ.* 1995;73(1):115–121.
3. Quigley HA. Glaucoma. *Lancet.* 2011;377(9774):1367–1377.
4. Foster PJ, Buhrmann R, Quigley HA, Johnson GJ. The definition and classification of glaucoma in prevalence surveys. *Br J Ophthalmol.* 2002;86(2):238–242.
5. Kwon YH, Fingert JH, Kuehn MH, Alward WL. Primary open-angle glaucoma. *N Engl J Med.* 2009;360(11):1113–1124.
6. Leske MC, Heijl A, Hussein M, Bengtsson B, Hyman L, Komaroff E. Factors for glaucoma progression and the effect of treatment: the early manifest glaucoma trial. *Arch Ophthalmol.* 2003;121(1):48–56.
7. Anderson DR, Normal Tension Glaucoma Study. Collaborative normal tension glaucoma study. *Curr Opin Ophthalmol.* 2003;14(2):86–90.
8. Gordon MO, Beiser JA, Brandt JD, et al. The Ocular Hypertension Treatment Study: baseline factors that predict the onset of primary open-angle glaucoma. *Arch Ophthalmol.* 2002;120(6):714–720; discussion 829–830.
9. Kass MA, Heuer DK, Higginbotham EJ, et al. The Ocular Hypertension Treatment Study: a randomized trial determines that topical ocular hypotensive medication delays or prevents the onset of primary open-angle glaucoma. *Arch Ophthalmol.* 2002;120(6):701–713; discussion 829–830.
10. Collaborative Normal-Tension Glaucoma Study Group. Comparison of glaucomatous progression between untreated patients with normal-tension glaucoma and patients with therapeutically reduced intraocular pressures. *Am J Ophthalmol.* 1998;126(4):487–497.
11. Collaborative Normal-Tension Glaucoma Study Group. The effectiveness of intraocular pressure reduction in the treatment of normal-tension glaucoma. *Am J Ophthalmol.* 1998;126(4):498–505.
12. Morrison JC, L'Hernault NL, Jerdan JA, Quigley HA. Ultrastructural location of extracellular matrix components in the optic nerve head. *Arch Ophthalmol.* 1989;107(1):123–129.
13. Quigley HA, Brown AE, Morrison JD, Drance SM. The size and shape of the optic disc in normal human eyes. *Arch Ophthalmol.* 1990;108(1):51–57.
14. Anderson DR. Ultrastructure of human and monkey lamina cribrosa and optic nerve head. *Arch Ophthalmol.* 1969;82(6):800–814.
15. Coudrillier B, Tian J, Alexander S, Myers KM, Quigley HA, Nguyen TD. Biomechanics of the human posterior sclera: age- and glaucoma-related changes measured using inflation testing. *Invest Ophthalmol Vis Sci.* 2012;53(4):1714–1728.
16. Hommer A, Fuchsjaeger-Mayrl G, Resch H, Vass C, Garhofer G, Schmetterer L. Estimation of ocular rigidity based on measurement of pulse amplitude using pneumotonometry and fundus pulse using laser interferometry in glaucoma. *Invest Ophthalmol Vis Sci.* 2008;49(9):4046–4050.
17. Zode GS, Sethi A, Brun-Zinkernagel AM, Chang IF, Clark AF, Wordinger RJ. Transforming growth factor- β 2 increases extracellular matrix proteins in optic nerve head cells via activation of the Smad signaling pathway. *Mol Vis.* 2011;17:1745–1758.
18. Pena JD, Taylor AW, Ricard CS, Vidal I, Hernandez MR. Transforming growth factor β isoforms in human optic nerve heads. *Br J Ophthalmol.* 1999;83(2):209–218.
19. Agarwal P, Daher AM, Agarwal R. Aqueous humor TGF- β 2 levels in patients with open-angle glaucoma: a meta-analysis. *Mol Vis.* 2015;21:612–620.
20. Buscemi L, Ramonet D, Klingberg F, et al. The single-molecule mechanics of the latent TGF- β 1 complex. *Curr Biol.* 2011;21(24):2046–2054.

21. Hinz B. The extracellular matrix and transforming growth factor- β 1: tale of a strained relationship. *Matrix Biol.* 2015;47:54–65.
22. Klingberg F, Chow ML, Koehler A, et al. Prestress in the extracellular matrix sensitizes latent TGF- β 1 for activation. *J Cell Biol.* 2014;207(2):283–297.
23. Neelisetty S, Alford C, Reynolds K, et al. Renal fibrosis is not reduced by blocking transforming growth factor- β signaling in matrix-producing interstitial cells. *Kidney Int.* 2015;88(3):503–514.
24. Zheng B, Zhang Z, Black CM, de Crombrughe B, Denton CP. Ligand-dependent genetic recombination in fibroblasts: a potentially powerful technique for investigating gene function in fibrosis. *Am J Pathol.* 2002;160(5):1609–1617.
25. Schlecht A, Leimbeck SV, Tamm ER, Braunger BM. Tamoxifen-containing eye drops successfully trigger Cre-mediated recombination in the entire eye. *Adv Exp Med Biol.* 2016;854:495–500.
26. Ito YA, Belforte N, Cueva Vargas JL, Di Polo A. A magnetic microbead occlusion model to induce ocular hypertension-dependent glaucoma in mice. *J Vis Exp.* 2016;(109):e53731.
27. Icare Finland Oy. Icare TONOLAB user's and maintenance manual. Available at: https://tonovet.com/wp-content/uploads/2015/12/TONOLAB_manual_2.2_EN.pdf. Accessed January 23, 2024.
28. Fuchshofer R, Yu AH, Welge-Lussen U, Tamm ER. Bone morphogenetic protein-7 is an antagonist of transforming growth factor- β 2 in human trabecular meshwork cells. *Invest Ophthalmol Vis Sci.* 2007;48(2):715–726.
29. Koschade SE, Koch MA, Braunger BM, Tamm ER. Efficient determination of axon number in the optic nerve: a stereological approach. *Exp Eye Res.* 2019;186:107710.
30. Jobling AI, Gentle A, Metlapally R, McGowan BJ, McBrien NA. Regulation of scleral cell contraction by transforming growth factor- β and stress: competing roles in myopic eye growth. *J Biol Chem.* 2009;284(4):2072–2079.
31. Jobling AI, Nguyen M, Gentle A, McBrien NA. Isoform-specific changes in scleral transforming growth factor- β expression and the regulation of collagen synthesis during myopia progression. *J Biol Chem.* 2004;279(18):18121–18126.
32. Gentle A, Liu Y, Martin JE, Conti GL, McBrien NA. Collagen gene expression and the altered accumulation of scleral collagen during the development of high myopia. *J Biol Chem.* 2003;278(19):16587–16594.
33. Marcus MW, de Vries MM, Junoy Montolio FG, Jansonius NM. Myopia as a risk factor for open-angle glaucoma: a systematic review and meta-analysis. *Ophthalmology.* 2011;118(10):1989–1994.e2.
34. Jonas JB, Panda-Jonas S, Wang YX. Glaucoma neurodegeneration and myopia. *Prog Brain Res.* 2020;257:1–17.
35. Tan NYQ, Sng CCA, Jonas JB, Wong TY, Jansonius NM, Ang M. Glaucoma in myopia: diagnostic dilemmas. *Br J Ophthalmol.* 2019;103(10):1347–1355.
36. Cousins SW, McCabe M, Danielpour D, Streilein JW. Transforming growth-factor-beta (TGF-beta) is an immunosuppressive molecule in aqueous humor. *FASEB J.* 1991;5(4):A628–A628.
37. Pasquale LR, Dormanpease ME, Luttly GA, Quigley HA, Jampel HD. Immunolocalization of TGF-beta-1, TGF-beta-2, and TGF-beta-3 in the anterior segment of the human eye. *Invest Ophthalmol Vis Sci.* 1993;34(1):23–30.
38. Jampel HD, Roche N, Stark WJ, Roberts AB. Transforming growth factor- β in human aqueous humor. *Curr Eye Res.* 1990;9(10):963–969.
39. Braunger BM, Leimbeck SV, Schlecht A, Volz C, Jägle H, Tamm ER. Deletion of ocular transforming growth factor β signaling mimics essential characteristics of diabetic retinopathy. *Am J Pathol.* 2015;185(6):1749–1768.
40. Braunger BM, Pielmeier S, Demmer C, et al. TGF- β signaling protects retinal neurons from programmed cell death during the development of the mammalian eye. *J Neurosci.* 2013;33(35):14246–14258.
41. Schlecht A, Leimbeck SV, Jägle H, Feuchtinger A, Tamm ER, Braunger BM. Deletion of endothelial transforming growth factor- β signaling leads to choroidal neovascularization. *Am J Pathol.* 2017;187(11):2570–2589.
42. Quigley HA, Pitha IF, Welsbie DS, et al. Losartan treatment protects retinal ganglion cells and alters scleral remodeling in experimental glaucoma. *PLoS One.* 2015;10(10):e0141137.
43. Bar-Klein G, Cacheaux LP, Kamintsky L, et al. Losartan prevents acquired epilepsy via TGF- β signaling suppression. *Ann Neurol.* 2014;75(6):864–875.
44. Wu M, Peng Z, Zu C, et al. Losartan attenuates myocardial endothelial-to-mesenchymal transition in spontaneous hypertensive rats via inhibiting TGF- β /Smad signaling. *PLoS One.* 2016;11(5):e0155730.
45. Yang H, Hirooka K, Fukuda K, Shiraga F. Neuroprotective effects of angiotensin II type 1 receptor blocker in a rat model of chronic glaucoma. *Invest Ophthalmol Vis Sci.* 2009;50(12):5800–5804.